

Dimethyl itaconate inhibits LPS-induced microglia inflammation and inflammasome-mediated pyroptosis via inducing autophagy and regulating the Nrf-2/HO-1 signaling pathway

SU YANG¹, XINGXING ZHANG², HENGLI ZHANG¹, XIANGXIANG LIN¹, XIJUN CHEN¹,
YING ZHANG¹, XIAO LIN¹, LIJIE HUANG¹ and QICHUAN ZHUGE¹

¹Zhejiang Provincial Key Laboratory of Aging and Neurological Disorder Research, Department of Neurosurgery,

²Department of Operation Room, The First Affiliated Hospital of Wenzhou Medical University,
Wenzhou, Zhejiang 325000, P.R. China

Received February 2, 2021; Accepted June 10, 2021

DOI: 10.3892/mmr.2021.12311

Abstract. The endogenous metabolite itaconate and its cell-permeable derivative dimethyl itaconate (DI) have been identified as anti-inflammatory regulators of macrophages; however, their contribution to inflammasome-mediated pyroptosis remains unknown. The present study examined the molecular mechanism of DI on NLR family pyrin domain-containing 3 (NLRP3) inflammasome assembly and NLRP3 inflammasome-dependent pyroptosis in microglia. Lipopolysaccharide (LPS) and ATP were used to induce microglia pyroptosis *in vitro*; this process was confirmed by TUNEL assay, lactate dehydrogenase (LDH) detection and gasdermin D (GSDMD) expression analysis. The regulation of microglia polarization and inflammatory cytokine expression was assessed by immunofluorescence assays and ELISA. To investigate the associated mechanism of action, the expression levels of the nuclear factor erythroid 2-related factor 2 (Nrf-2)/heme oxygenase-1 (HO-1) pathway proteins were analyzed by western blotting. Finally, the regulatory effect of DI on autophagy and its association with inflammation was determined by western blotting. The present study demonstrated that DI administration inhibited NLRP3 assembly, LDH release and GSDMD cleavage. Cotreatment of DI with LPS and ATP facilitated the transition from M1 to M2, reduced inflammatory mediator expression and impeded NF- κ B phosphorylation. In addition, DI effectively reduced

reactive oxygen species production through the Nrf-2/HO-1 pathway. Moreover, DI induced cellular autophagy, whereas inhibition of autophagy with 3-methyladenine markedly reversed its inhibitory effect on NLRP3-dependent pyroptosis. Taken together, the present study suggested that DI participated in the Nrf-2/HO-1 pathway and served a key role in microglia inflammation and NLRP3 inflammasome-mediated pyroptosis via induction of autophagy.

Introduction

Microglia are innate immune cells resident in the central nervous system; notably, microglia have a role in the inflammatory defense system stimulated by infection and environmental pathogens (1,2). Microglia interact with neurons, astrocytes and blood vessels in their quiescent state, and constantly scavenge damaged neurons and pathogens. Microglia can be activated to transition from the quiescent to the active state in response to brain injury or inflammatory stimuli, such as systemic infection, cerebral ischemia, hemorrhagic stroke and traumatic brain injury (3,4). In their pro-inflammatory state (M1), microglia release various cytokines (IL-6, IL-1 β and TNF- α) that combat pathogenic infection; however, prolonged activation of the M1 state can cause inflammatory damage to peripheral cells and lead to neuronal cell death (5). Microglia have a neuroprotective function in their anti-inflammatory state (M2) via the expression of anti-inflammatory cytokines and other factors (6). Therefore, the induction of M1 to M2 phenotype transition may be an effective strategy for combating neurological damage.

To assess the initiation of inflammatory processes, the expression levels of key inflammatory molecules can be evaluated. The inflammasome is a multicomponent protein complex that triggers innate immune responses by activation of specific proteins, such as NLR family pyrin domain-containing (NLRP)1, NLRP3, NLR family CARD domain-containing 4 and absent in melanoma 2 (7); among these proteins, the NLRP3 inflammasome has received considerable attention due to its unique role in the inflammatory response and associated types of cell death (8,9). The NLRP3 inflammasome

Correspondence to: Dr Lijie Huang or Dr Qichuan Zhuge, Zhejiang Provincial Key Laboratory of Aging and Neurological Disorder Research, Department of Neurosurgery, The First Affiliated Hospital of Wenzhou Medical University, 1 Fanhai West Road, Ouhai, Wenzhou, Zhejiang 325000, P.R. China
E-mail: lijiehuangwy@163.com
E-mail: qc.zhuge@wmu.edu.cn

Key words: dimethyl itaconate, microglia polarization, NLR family pyrin domain-containing 3 inflammasome, pyroptosis, autophagy

can be activated by numerous pathogen-associated molecular patterns (PAMPs) or endogenous danger-associated molecular patterns (DAMPs) (10), such as reactive oxygen species (ROS) (11), mitochondrial DNA and aggregated peptide (12). A previous study confirmed that lipopolysaccharide (LPS) can initiate a priming step via induction of NF- κ B and can trigger secondary activation of the NLRP3 inflammasome (13).

Pyroptosis was initially identified as caspase-1-dependent inflammasome-mediated programmed necrosis (14). Pyroptosis is a lytic process, which is distinct from apoptosis and other types of programmed cell death (15), and is associated with cell swelling and large bubbles emanating from the plasma membrane (16). It has been reported that pyroptosis is initiated by NLRP3 inflammasome assembly and is terminated with gasdermin D (GSDMD) cleavage, which is in turn accompanied by the release of mature IL-18 and IL-1 β (10,17). NLRP3 polymerizes with cleaved caspase-1 via the apoptosis-associated speck-like protein-containing CARD adaptor, leading to cleavage of the inflammatory cytokines IL-18 and IL-1 β into their mature forms (18). Activated caspase-1 subsequently cleaves GSDMD (19), thus releasing its N- and C-domains. The N-domain of GSDMD forms membrane pores and releases mature IL-1 β and IL-18 into the extracellular space, causing a severe inflammatory cascade reaction (20).

It has been reported that inflammatory stimuli induce immune responsive gene 1 (*Irg-1*) expression, which in turn catalyzes the production of itaconate from the tricarboxylic acid (TCA) cycle. Notably, *Irg-1* is highly expressed in LPS-activated macrophages (21,22). Itaconate affects macrophage metabolism and the inflammatory response by inhibiting succinate dehydrogenase (SDH) (23-25). Upon inhibition of SDH-derived ROS, itaconate exerts its anti-inflammatory effects on macrophage activation following ischemia-reperfusion injury. Using *Irg-1*^{-/-} mice, Lampropoulou *et al* (23) demonstrated that itaconate was a major physiological regulator of succinate metabolism, mitochondrial respiration and inflammatory cytokine expression. Recently, it has been shown that itaconate and its membrane-permeable derivative dimethyl itaconate (DI) can selectively inhibit the expression of several cytokines (26,27), including IL-6 and IL-12. However, the inhibition of SDH is not sufficient to account for the prominent immunoregulatory effect of DI (22,28). Mills *et al* (28) revealed that itaconate can directly increase nuclear factor erythroid 2-related factor 2 (Nrf-2) expression via alkylation of the cysteine residues of Kelch-like ECH-associated protein 1 (KEAP1), a covalent inhibitor of Nrf-2. This may consequently result in the induction of downstream antioxidant and anti-inflammatory gene expression (29). However, the function of this biochemical pathway in microglial cells and its precise role in pyroptosis remains unknown. The present study evaluated the ability of DI to prevent pyroptosis via modulation of the inflammatory response, microglia polarization, and the regulation of Nrf-2 expression and autophagy.

Materials and methods

Reagents and antibodies. The cell culture reagents were purchased from Gibco; Thermo Fisher Scientific, Inc. The

antibodies against GSDMD (1:1,000; cat. no. ab209845), caspase-1 (p20) (1:500; cat. no. ab1872), IL-1 β (1:1,000; cat. no. ab9722), autophagy-related (ATG)-5 (1:1,000; cat. no. ab199560), Beclin-1 (1:1,000; cat. no. ab62557), heme oxygenase-1 (HO-1; 1:1,000; cat. no. ab137749) and β -actin (1:1,000; cat. no. ab8227) were purchased from Abcam. The antibodies against NLRP3 (1:1,000; cat. no. 13158), P62 (1:1,000; cat. no. 13121S), and LC3B (1:1,000; cat. no. 2775) were obtained from Cell Signaling Technology, Inc. The antibodies against NF- κ B p65 (1:1,000; cat. no. 14220-1) and Nrf-2 (1:1,000; cat. no. 16396-1) were purchased from ProteinTech Group, Inc., and the antibodies against phosphorylated (p)-NF- κ B p65 (Ser536) (1:1,000; cat. no. AF2006) and Nucleolin (1:1,000; cat. no. DF12542) were purchased from Affinity Biosciences. DI was purchased from Sigma-Aldrich; Merck KGaA. DAPI and other reagents were obtained from Beyotime Institute of Biotechnology.

Cell culture. BV2 microglial cells were purchased from iCell Bioscience Inc., (cat. no. iCell-m011). The cells were cultured in DMEM (Gibco; Thermo Fisher Scientific, Inc.) supplemented with 10% FBS (Gibco; Thermo Fisher Scientific, Inc.) and penicillin (100 U/ml)/streptomycin (100 U/ml) with 5% CO₂ at 37°C. LPS, VX765 and 3-methyladenine (3-MA) were obtained from MedChemExpress. ATP was purchased from Beyotime Institute of Biotechnology. Sham group were only treated with the same volume of PBS. To effectively induce cellular inflammation, 6-h treatment at 37°C with LPS (1.5 μ g/ml) was selected, and DI (0-200 μ M) and VX765 (10 μ M; inhibitor of pyroptosis) were added simultaneously. ATP (3 mM) was added for an additional 1 h prior to cell lysis or imaging to trigger pyroptosis *in vitro*. If necessary, 5 mM 3-MA pretreatment was performed 2 h prior to LPS treatment to inhibit autophagy.

Morphological analysis. BV2 microglial cells were digested and incubated in a 6-well plate overnight. After treatment with LPS (1.5 μ g/ml) and DI (200 μ M) at 37°C for 5 h, ATP (3 mM) was added for an additional 1 h to trigger pyroptosis *in vitro*. The microglia morphology was analyzed using a fluorescence microscope (DMI8; Leica Microsystems, Inc.).

Animals and ethics guidelines. A total of five male C57BL/6 mice (age, 1-3 days; weight, 1-2 g) were obtained from two pregnant female mice, which were purchased from the Animal Centre of Wenzhou Medical University (Wenzhou, China). The pregnant mice were maintained in specific pathogen-free conditions at room temperature with 60% relative humidity, under a 12-h light/dark cycle with free access to food and water. The present study was conducted in accordance with the ARRIVE guidelines for the Care and Use of Laboratory Animals (25), and the experimental procedures were approved by the Ethics Committee of Wenzhou Medical University (approval no. wyd2019-0598). All efforts were made to minimize suffering. Newborn mice were euthanized via the administration of CO₂ at 30% volume displacement rate. Lack of heartbeat and long-term unconsciousness were used to confirm animal death. Subsequently, mice were placed in 75% ethyl alcohol for disinfection and primary microglia extraction.

Primary microglia culture. Newborn (1-3 days old) C57BL/6 mice, after euthanasia with CO₂, were decapitated and the heads were quickly placed into a petri dish with 3-5 ml ice-cold DMEM. Following removal of the meninges and blood vessels, the tissues were cut, digested and passed through a cell filter screen (40- μ m nylon mesh). The obtained samples were centrifuged at 300 x g at 4°C for 5 min, and the resulting cell pellet was reconstituted in DMEM with 10% FBS and penicillin/streptomycin under standard conditions. The microglial cells were allowed to proliferate for 10-12 days and reached 90% confluence. Subsequently, they were isolated by mild trypsinization and seeded in new culture plates for further experiments. For further verification of the anti-pyroptosis activity of DI against ATP and LPS-induced pyroptosis, microglia was treated with LPS (1.5 μ g/ml) and DI (200 μ M) for 5 h at 37°C, and 3 mM ATP was added for an additional 1 h prior to cell lysis.

Cell viability assay. Cell viability was measured using the MTT assay. Briefly, BV2 microglial cells (5x10³/well) were digested and incubated in a 96-well plate overnight prior to DI treatment (50, 100, 150, 200 or 250 μ M) for 6 or 12 h. Subsequently, 50 μ l MTT solution (1 mg/ml) was added to each well and was continuously incubated at 37°C for 4 h. Following incubation, the supernatant was removed carefully and the insoluble formazan was dissolved in 150 μ l DMSO. The absorbance was measured at 570 nm to assess cell viability.

TUNEL assay. TUNEL assays were performed using a Colorimetric TUNEL Apoptosis Assay kit (Beyotime Institute of Biotechnology) according to the manufacturer's instructions. The cells were fixed with 4% paraformaldehyde at room temperature for 15 min, incubated with 50 μ l TUNEL detection mixture at 37°C for 1 h in the dark and rinsed in PBS. Cyanine 3-labeled dUTP was applied to stain apoptotic cells, and DAPI was used for nuclear staining. Images of cells were captured using a fluorescence microscope (DMI8; Leica Microsystems, Inc.).

Western blot analysis. The cells were collected and lysed using RIPA lysis buffer (cat. no. 89901; Thermo Fisher Scientific, Inc.) to extract total cellular proteins. The protein concentration was determined with a BCA protein assay kit (cat. no. 23225; Pierce; Thermo Fisher Scientific, Inc.). Equal amounts of protein (30 μ g) were separated by SDS-PAGE on 12% gels and were subsequently transferred onto PVDF membranes (MilliporeSigma). After blocking with 5% milk at room temperature for 2 h, the membranes were incubated with primary antibodies at 4°C overnight. Subsequently, the membranes were washed three times and incubated with HRP-linked anti-rabbit IgG secondary antibody (cat. no. 7074s; 1:5,000; Cell Signaling Technology, Inc.) at room temperature for 1 h. Finally, the bands were visualized using ECL Reagents (Advansta, Inc.) and analyzed by ImageJ software (version 1.51; National Institutes of Health).

Lactate dehydrogenase (LDH), malondialdehyde (MDA) and SDH activity detection. To detect LDH release, the medium was collected from the cell cultures following drug treatment and the OD was measured at 450 nm using LDH detection kits

(Beijing Solarbio Science & Technology Co., Ltd.) according to the manufacturer's instructions. To detect MDA content, the cells were lysed in RIPA buffer (Thermo Fisher Scientific, Inc.) on ice for 30 min. Following centrifugation at 12,000 x g at 4°C for 10 min, 100 μ l supernatant was fixed with 200 μ l MDA working reagent and boiled for 15 min. The absorbance was detected at 532 nm using the Lipid Peroxidation MDA Assay kit (Beyotime Institute of Biotechnology) according to the manufacturer's instructions. To detect SDH activity, cells were lysed and centrifuged at 12,000 x g at 4°C for 10 min. The supernatant was collected and the OD was detected at 600 nm using the SDH activity detection kit (Beijing Solarbio Science & Technology Co., Ltd.) according to the manufacturer's instructions.

RNA extraction from microglial cells and reverse transcription-quantitative PCR (RT-qPCR). Total RNA was isolated from BV2 cells using TRIzol[®] reagent (Invitrogen; Thermo Fisher Scientific, Inc.) and cDNA was obtained with a RevertAid First Strand cDNA Synthesis kit (cat. no. K1622; Thermo Fisher Scientific, Inc.). qPCR was performed with SYBR Premix Ex Taq (Bio-Rad Laboratories, Inc.). The thermocycling conditions were set as follows: Initial denaturation at 95°C for 30 sec, followed by annealing and elongation for 40 cycles at 95°C for 15 sec, 60°C for 30 sec and 72°C for 30 sec, and a final extension at 72°C for 2 min. Relative quantification was calculated using the 2^{- $\Delta\Delta$ C_q} method (30). The primers used are listed in Table I; primers were synthesized by Sangon Biotech Co., Ltd. GAPDH was used as the internal reference gene for comparison.

ELISA for determination of cytokine levels. The levels of cytokines were determined using specific ELISA kits. BV2 microglial cells were seeded into 25-cm² culture flasks at a density of 1x10⁵ cells/well. After treatment, the cells were collected and homogenized in ice-cold PBS. Following centrifugation at 12,000 x g at 4°C for 10 min, the supernatant was collected, and the samples were analyzed to detect inducible nitric oxide synthase (iNOS) (cat. no. BP-E20450; Shanghai Boyun Biotech Co., Ltd.), TNF- α (cat. no. BMS607-2INST; Thermo Fisher Scientific, Inc.), IL-6 (cat. no. BMS603-2; Thermo Fisher Scientific, Inc.), IL-18 (cat. no. BMS618-3; Thermo Fisher Scientific, Inc.), IFN- γ (cat. no. BMS606-2; Thermo Fisher Scientific, Inc.) and IL-10 (cat. no. BMS614INST; Thermo Fisher Scientific, Inc.) levels in accordance with the manufacturer's protocols. The OD was measured at 450 nm on a microplate reader (Spectra MAX 190; Molecular Devices, LLC).

Immunofluorescence staining. The treated microglial cells were fixed with 4% paraformaldehyde at room temperature for 30 min and subsequently permeabilized with 0.2% Triton X-100. Following blocking with 10% donkey serum (Sigma-Aldrich; Merck KGaA) and 0.2% Triton X-100 at room temperature for 2 h, the samples were incubated at 4°C for 24 h with primary antibodies against IBA-1 (1:200; cat. no. ab5076; Abcam), iNOS (1:200; cat. no. ab15323; Abcam), CD206 (1:200; cat. no. ab8918; Abcam) and p-NF- κ B p65 (Ser536) (1:200; cat. no. AF2006; Affinity Biosciences), followed by incubation with respective secondary antibodies at 37°C for

Table I. Primers used for reverse-transcription quantitative PCR.

Gene	Forward primer 5'-3'	Reverse primer 5'-3'
<i>IL-1β</i>	GTGTCTTTCCCGTGGACCTTC	TCATCTCGGAGCCTGTAGTGC
<i>TNF-α</i>	CTCCAGGCGGTGCCTATGTCT	CTCCTCCACTTGGTGGTTTGC
<i>IL-18</i>	TGTCAGAAGACTCTTGCGTCAA	TATTCGCTATTACTGCGGTTGT
<i>IL-4</i>	TTGAACGAGGTACAGGAGAAG	CTTGGAAGCCCTACAGACGAG
<i>iNOS</i>	AGGGAATCTTGGAGCGAGTTG	CGTAATGTCCAGGAAGTAGGTGAG
<i>Arg-1</i>	TGCCAGACGGAAGGACCATT	CCAGCACGAAGGTCTCGATGT
<i>Irg-1</i>	GATGGTATCATTCGGAGGAGC	CTGGAGGTGTTGGAAGTGTAGAT
<i>MCP-1</i>	TGCATCTGCCCTAAGGTCTTC	AGTGCTTGAGGTGGTTGTGGA
<i>NLRP3</i>	GTGGATGGGTTTGCTGGGATA	TGCGTGTAGCGACTGTTGAGG
<i>NLRP1</i>	CTCTTTATCTTGGTTCCCGCTAT	GTGCCTCTTGTCTTTGATTTC
<i>AIM2</i>	GAATCTAACCACGAAGTCCCA	ACCAACACCTCCATTGTCCCT
<i>GAPDH</i>	GCCAAGGCTGTGGGCAAGGT	TCTCCAGGCGGCACGCAGA

AIM2, absent in melanoma 2; Arg-1, arginase-1; iNOS, inducible nitric oxide synthase; Irg-1, immune responsive gene 1; MCP-1, monocyte chemoattractant protein 1; NLRP, NLR family pyrin domain-containing.

1 h, including 488-conjugated donkey anti-goat antibody (1:500; cat. no. E032231-02; Canlifesci, Inc.), 594-conjugated donkey anti-mouse antibody (1:500; cat. no. E032411-02; Canlifesci, Inc.), and 594-conjugated donkey anti-rabbit antibody (1:500; cat. no. E032421-01; Canlifesci, Inc.). Finally, the cells were stained with DAPI (cat. no. C1002; Beyotime Institute of Biotechnology) at room temperature for 10 min and subsequently examined with a scanning fluorescence microscope (DMi8; Leica Microsystems, Inc.).

Gene knockdown with small interfering RNA (siRNA). The cells were transfected using the riboFECT CP transfection reagent (cat. no. C10511-05; Guangzhou RiboBio Co., Ltd.) according to the manufacturer's instructions. Briefly, BV2 cells were seeded into 6-well plates at a density of 1×10^6 cells/well. siRNA (1.25 μ l) was diluted with 30 μ l riboFECTTM CP Buffer, and mixed with 3 μ l riboFECTTM CP reagent to form the transfection complex. Subsequently, the cells were transfected with the mixture containing 100 nM siRNA-Nrf-2 (Guangzhou RiboBio Co., Ltd.) (three targeted sequences: siRNA-Nrf-2-1, 5'-GCAGGAGAGGTAAGAATAA-3'; siRNA-Nrf-2-2, 5'-GCACAATGGAATTCAATGA-3'; and siRNA-Nrf-2-3, 5'-CGACAGAAACCTCCATCTA-3') or 100 nM siRNA-NLRP3 (Guangzhou RiboBio Co., Ltd.) (three targeted sequences: siRNA-NLRP3, 5'-GTACTTAAATCGTGAAACA-3'; siRNA-NLRP3-2, 5'-CAGCCAGAGTGG AATGACA-3'; siRNA-NLRP3-3, 5'-GGATGGCTTTGATGA GCTA-3'), and incubated in 2 ml DMEM for 48 h at 37°C. Scrambled siRNA (targeted sequence, 5'-GGCTCTAGAAAA GCCTATGC-3'; Guangzhou RiboBio Co., Ltd.) was used as the negative control. The transfection efficiency of the siRNA-Nrf-2 was assessed by western blot analysis, whereas the transfection efficiency of the siRNA-NLRP3 was assessed by RT-qPCR. The siRNA with the most effective silencing efficiency was used for further experiments. The transfected cells were immediately treated with drugs within 24 h for investigation.

Flow cytometric analysis of ROS. ROS production was determined using 2,7-dichlorodihydrofluorescein diacetate (DCFH-DA; cat. no. S0033S; Beyotime Institute of Biotechnology) according to the manufacturer's protocol. After drug treatment, the culture medium was discarded and the cells were incubated with 10 μ M DCFH-DA for 10 min at 37°C. After washing away the unbound DCFH-DA, the cells were collected and resuspended in DMEM for ROS detection. Cellular ROS was detected using a flow cytometer (CytoFLEX LX; Beckman Coulter, Inc.), and analyzed via FlowJo software (version 10; FlowJo LLC).

Statistical analysis. All experiments were repeated three times and all data were analyzed using GraphPad Prism 5.0 (GraphPad Software, Inc.) or SPSS 22.0 (IBM Corporation) and presented as the mean \pm SD. An unpaired Student's t-test was applied to analyze the comparisons between two groups. One-way ANOVA followed by Tukey's post hoc test was used to compare data from the different groups. $P < 0.05$ was considered to indicate a statistically significant difference.

Results

DI is not cytotoxic at specific concentrations in BV2 microglial cells. DI is a novel membrane-permeable derivative of itaconate (Fig. 1A and B). The excessive production of itaconate may cause aberrant cell metabolism. Prior to the investigation of the biochemical effects of DI on microglial cells, its cytotoxicity was assessed using the MTT assay. Cell viability was assessed following DI treatment (50–250 μ M) for 6 or 12 h (Fig. 1C and D). The results demonstrated that cell viability was not significantly different in the treated groups compared with that in the sham group ($P < 0.05$). These findings indicated that DI did not exert cytotoxic effects against BV2 microglia at a concentration < 200 μ M. Based on these findings, DI was used in subsequent experiments at a concentration range between 0 and 200 μ M.

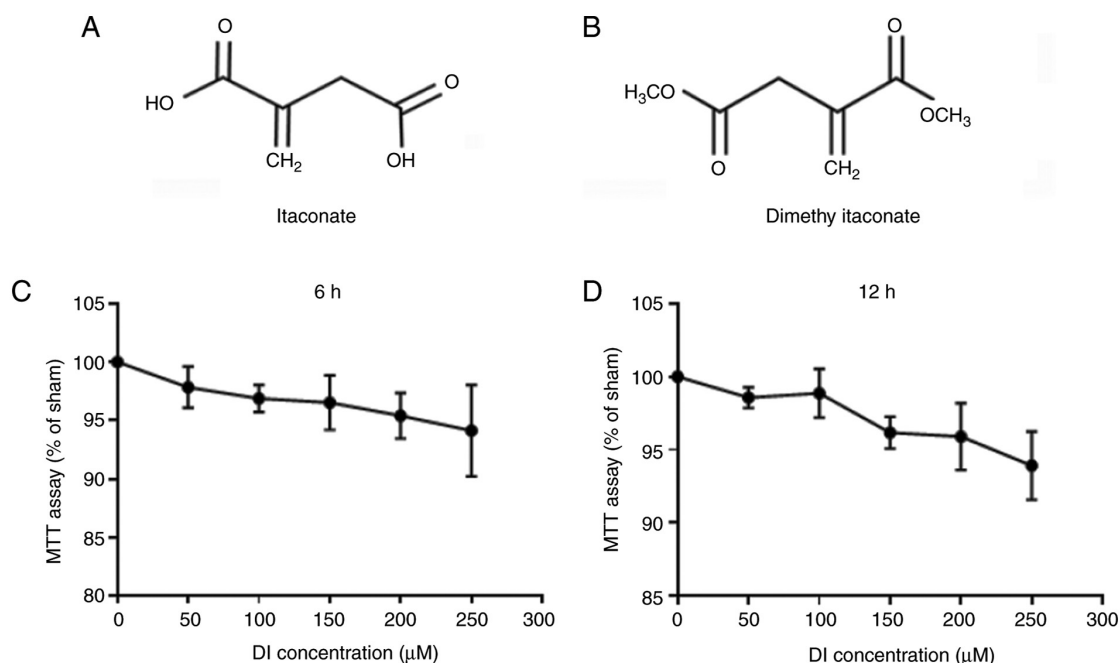


Figure 1. Effect of DI on the viability of BV2 microglia. Molecular structure of (A) itaconate and its derivative (B) DI. Cell viability under various doses of DI treatment for (C) 6 h and (D) 12 h were evaluated by MTT assay. Data are presented as the mean \pm standard error of the mean (n=3). DI, dimethyl itaconate.

DI protects BV2 cells against NLRP3-dependent canonical pyroptosis. Prior to investigation of the anti-inflammatory effects of DI in active microglia, the induction of *Irg-1* expression was assessed. The *Irg-1* gene encodes an enzyme, which catalyzes endogenous itaconate production under inflammatory conditions (in the present study following LPS stimulation). The results revealed that the expression levels of the *Irg-1* transcript were significantly increased following LPS and ATP stimulation (Fig. S1), which suggested the involvement of this enzyme in inhibition of inflammation.

Pyroptosis is a lytic, cell-swelling process, which is accompanied by GSDMD-mediated pore formation and secretion of the cell contents (16). The TUNEL assay indicated a higher number of apoptotic cells following LPS stimulation and ATP treatment of the cells. These effects were accompanied by increased LDH secretion and GSDMD cleavage (Fig. 2A-F). These findings confirmed membrane perforation and GSDMD-mediated pyroptosis. Subsequently, the anti-pyroptotic effect of DI was investigated. Cotreatment with DI markedly reduced the induction of cell apoptosis, LDH secretion and GSDMD cleavage, reflecting the inhibitory effect of DI on GSDMD-mediated pyroptosis (Fig. 2A-F).

Pyroptosis inhibition was confirmed following DI administration; therefore, the intrinsic mechanism was examined. The detection of the transcriptional levels of NLRs indicated the inhibitory activities of DI on NLRP3 transcription (Fig. S2), which suggested the involvement of NLRP3-associated pathways in this process. The expression levels of NLRP3, cleaved caspase-1, pro-IL-1 β and cleaved IL-1 β were markedly increased following stimulation of the cells with LPS and ATP, while co-treatment with DI significantly decreased expression of NLRP3, cleaved caspase-1, pro-IL-1 β and cleaved IL-1 β (Fig. 3A-E). These findings indicated that DI inhibited the expression of NLRP3 and pro-IL-1 β , and prevented the

cleavage of caspase-1, which eventually resulted in decreased cleaved IL-1 β . In addition, knockdown of NLRP3 by siRNA interference significantly inhibited pro-IL-1 β expression and GSDMD cleavage compared with in the LPS+ATP group (Fig. S3A-F), suggesting that DI regulated pyroptosis in the BV2 cell line via the NLRP3-caspase-1-GSDMD-dependent canonical pathway.

In order to further confirm the anti-pyroptotic activity of DI, primary microglial cells were extracted and cultured. DI administration effectively inhibited NLRP3-mediated pyroptosis by reducing the expression levels of NLRP3 and pro-IL-1 β , and preventing cleavage of caspase-1 and GSDMD (Fig. 3F-K). This suggested the anti-pyroptotic activity of this compound in primary microglia.

DI regulates microglia polarization and cellular inflammation by inducing NF- κ B expression. To assess the effects of DI on microglia polarization, the present study examined the transcripts of M1 and M2 markers. M1-polarized microglia cells are iNOS-positive and induce pro-inflammatory mediator expression (5), whereas M2-polarized microglia cells are CD206-positive and induce anti-inflammatory mediator expression. The present study revealed that 100 μ M DI reduced the transcription of *iNOS*, *TNF- α* and monocyte chemoattractant protein 1, which was increased following stimulation of the cells with LPS and ATP. Concomitantly, the transcription of arginase 1 and *IL-4* was increased by DI (Fig. 4A), indicating inhibition of M1 polarization and induction of M2 polarization. Furthermore, a double-immunofluorescence staining assay was performed and the results indicated that the number of Iba-1⁺/iNOS⁺ cells in the DI-treated group was significantly lower than that in the LPS and ATP group (Fig. 4B and C). These findings suggested that DI inhibited LPS and ATP-induced M1 polarization in BV2 cells.

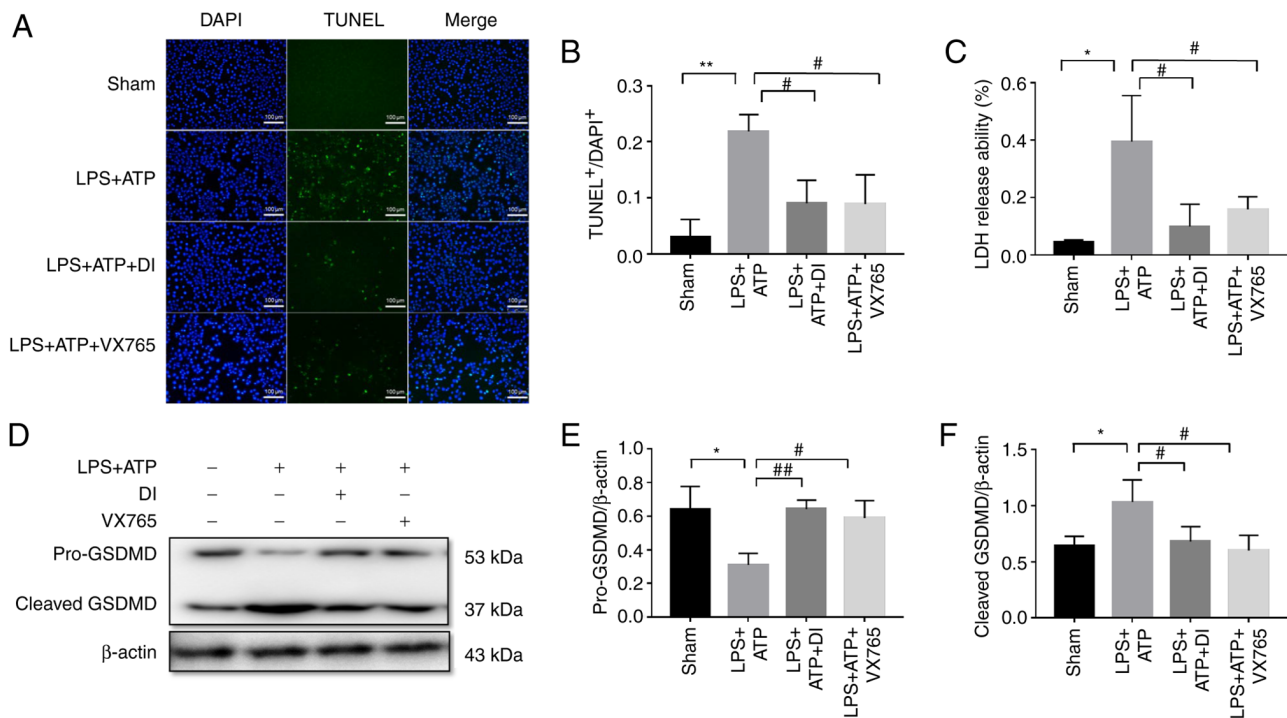


Figure 2. DI protects BV2 cells against GSDMD-mediated pyroptosis. (A) TUNEL assays were used to detect the apoptosis of BV2 cells stimulated with LPS and ATP in the presence or absence of DI or VX765. The apoptotic cells were stained with Cyanine 3-dUTP (green staining) and nuclei were counterstained with DAPI (blue staining). Scale bar, 100 μ m. (B) Statistical analysis of the TUNEL assay. (C) LDH release assay for detection of cell membrane pore formation. (D) Western blot analysis. Semi-quantification of (E) full-length GSDMD and (F) cleaved GSDMD stimulated by LPS and ATP in the presence or absence of DI or VX765. Data are presented as the mean \pm standard error of the mean (n=3). *P<0.05, **P<0.01 vs. sham group; #P<0.05, ##P<0.01 vs. LPS+ATP group. DI, dimethyl itaconate; GSDMD, gasdermin D; LDH, lactate dehydrogenase; LPS, lipopolysaccharide.

Moreover, DI treatment significantly increased the number of Iba-1⁺/CD206⁺ positive cells (Fig. 4D and E), which indicated that microglia were polarized to the M2 phenotype. Through detecting cellular morphology (Fig. S4A-C), it was demonstrated that LPS and ATP-stimulated microglia appeared with long synapses, whereas DI-treated microglia exhibited shorter synapses; however, more microglia were detected in the DI-treated group. These findings were in accordance with the classic morphology of microglia polarization, suggesting that DI may be a critical regulator of the transition from pro-inflammatory M1 to anti-inflammatory M2 polarization.

To elucidate the precise anti-inflammatory profile of DI, the levels of pro-inflammatory and anti-inflammatory mediators were detected. The levels of pro-inflammatory mediators, including iNOS, TNF- α , IL-6, IFN- γ and IL-18, which were induced by LPS and ATP stimulation, were significantly inhibited by DI (Fig. 5A-E), while anti-inflammatory cytokine IL-10 was largely induced by DI treatment (Fig. 5F). NF- κ B possesses a key priming role in LPS-induced inflammation (6). By detecting the phosphorylation of NF- κ B using immunofluorescence staining, it was revealed that LPS and ATP treatment promoted NF- κ B nuclear translocation, whereas DI administration effectively reduced these effects (Fig. 5G). In addition, western blotting was employed to assess the induction of NF- κ B phosphorylation following stimulation of the cells with LPS and ATP, it was found that cellular p-NF- κ B and nuclear p-NF- κ B were significantly increased (Fig. 5H-K). These effects were markedly inhibited by treatment of the cells with DI,

suggesting that this compound regulated the inflammatory response by inhibiting NF- κ B phosphorylation and nuclear translocation.

DI exerts cytoprotective effects via the Nrf-2/HO-1 pathway. Nrf-2 is the main transcription factor regulating the cytoprotective responses to oxidative and inflammatory stress. Following induction of oxidative and inflammatory stress, Nrf-2 is released from KEAP1, leading to its translocation to the nucleus, which initiates the expression of the downstream effector HO-1 (31). DI treatment significantly upregulated Nrf-2 and HO-1 expression levels in a dose-dependent manner compared with those in the sham group, indicating that the Nrf-2/HO-1 pathway contributed to cellular antioxidant activity (Fig. 6A-C).

To explore the association between the Nrf-2/HO-1 pathway and NLRP3-mediated pyroptosis, the expression of Nrf-2 was knocked down using siRNA interference (Fig. 6D and E). Treatment of the cells with DI induced the expression of HO-1; however, this effect was suppressed by the knockdown of Nrf-2 expression via transfection with siRNA (Fig. 6F and G). NLRP3, pro-IL-1 β and cleaved IL-1 β expression levels were reduced by treatment with DI, which was reversed by the knockdown of Nrf-2 expression (Fig. 6H-J), thus suggesting the protective effect of the Nrf-2/HO-1 pathway against inflammation.

ROS has been identified as a source of DAMPs, which trigger pyroptosis (32). Flow cytometric detection with DCFH-DA verified that DI could effectively inhibit LPS and

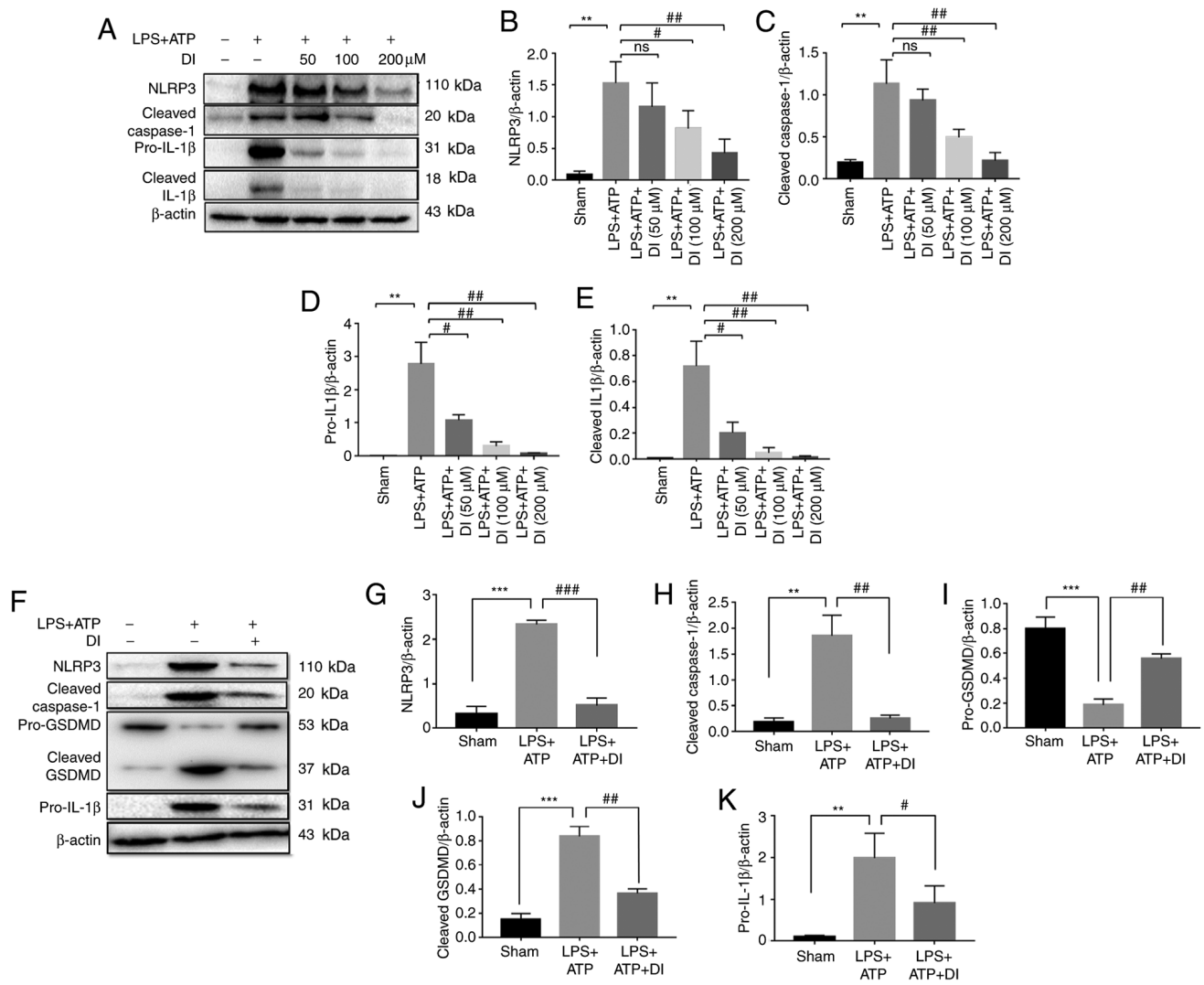


Figure 3. DI inhibits NLRP3-dependent pyroptosis in BV2 and primary microglia cells. (A) Western blot analysis. Semi-quantification of (B) NLRP3, (C) cleaved caspase-1 (p20), (D) pro-IL1β and (E) cleaved IL1β. (F) Western blot analysis. Semi-quantification of (G) NLRP3, (H) cleaved caspase-1, (I) pro-GSDMD, (J) cleaved GSDMD and (K) pro-IL-1β. Data are presented as the mean ± standard error of the mean (n=3). **P<0.01, ***P<0.001 vs. sham group; #P<0.05, ##P<0.01, ###P<0.001 vs. LPS+ATP group. DI, dimethyl itaconate; LPS, lipopolysaccharide; NLRP3, NLR family pyrin domain-containing 3; GSDMD, gasdermin D.

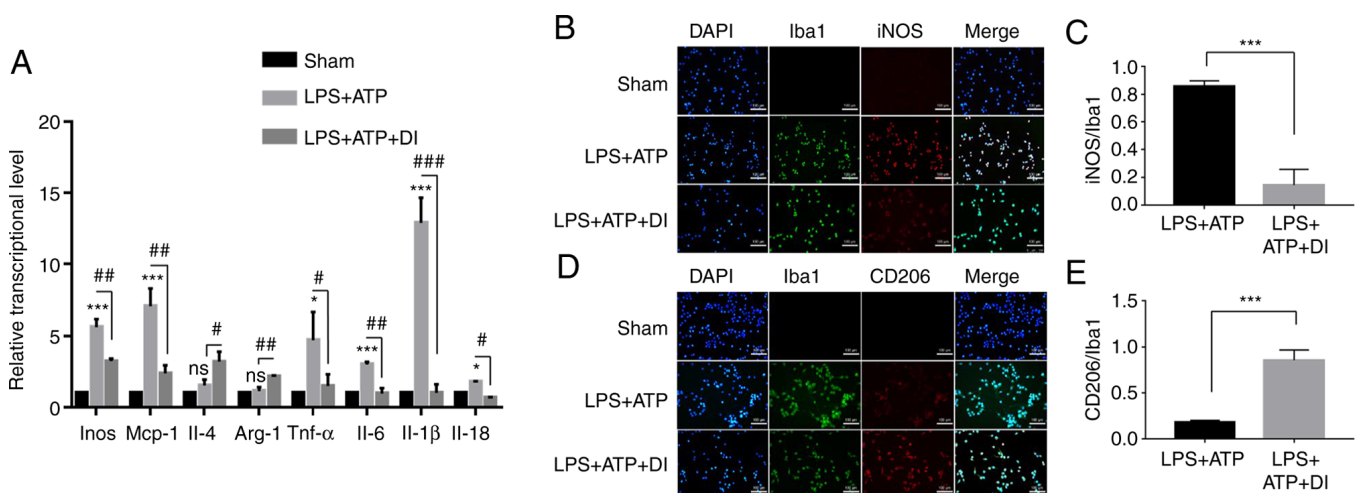


Figure 4. Regulatory role of DI on microglia polarization. (A) mRNA expression levels of *Inos*, *Mcp-1*, *Il-4*, *Arg-1*, *Tnf-α*, *Il-6*, *Il-1β* and *Il-18* as determined by reverse transcription-quantitative PCR. (B and C) Microglia M1 polarization (Iba1⁺/iNOS⁺) and (D and E) M2 polarization (Iba1⁺/CD206⁺) were determined by double-immunofluorescence assay. Scale bar, 100 μm. Data are presented as the mean ± standard error of the mean (n=3). *P<0.05, ***P<0.001 vs. sham group or as indicated; #P<0.05, ##P<0.01, ###P<0.001 vs. LPS+ATP group. Arg-1, arginase 1; DI, dimethyl itaconate; iNOS, inducible nitric oxide synthase; LPS, lipopolysaccharide; *Mcp-1*, monocyte chemoattractant protein 1.

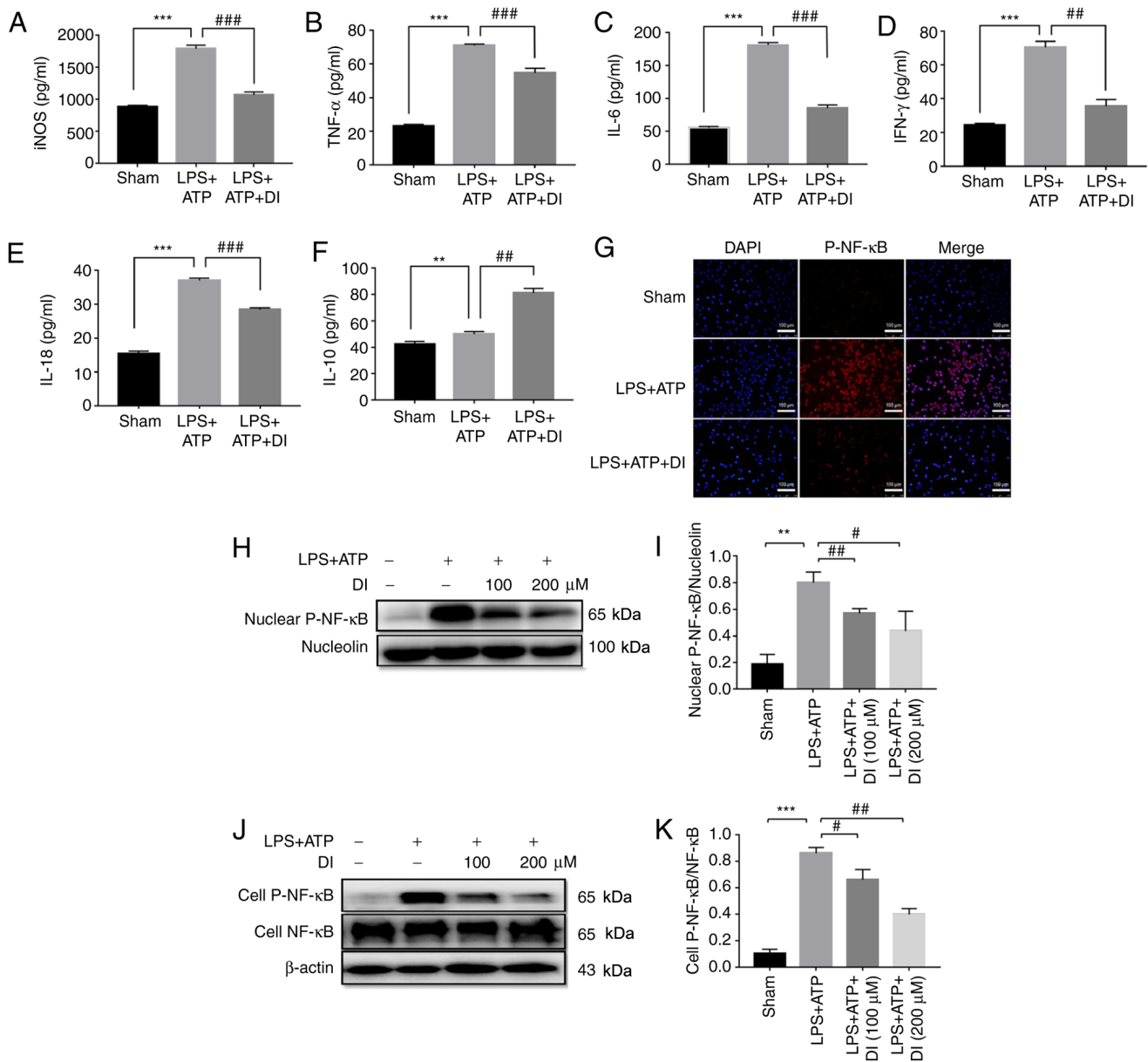


Figure 5. DI regulates microglia inflammatory profile via inhibiting NF- κ B phosphorylation and nuclear translocation. Levels of cytokines, including (A) iNOS, (B) TNF- α , (C) IL-6, (D) IFN- γ , (E) IL-18 and (F) IL-10, were determined by ELISA. (G) Nuclear translocation of p-NF- κ B was determined by immunofluorescence staining. Scale bar, 100 μ m. (H and I) p-NF- κ B expression in the nucleus were determined by western blotting. (J and K) Ratio of whole cell p-NF- κ B/total NF- κ B expression was determined by western blotting. Data are presented as the mean \pm standard error of the mean (n=3). **P<0.01, ***P<0.001 vs. sham group; #P<0.05, ##P<0.01, ###P<0.001 vs. LPS+ATP group. DI, dimethyl itaconate; iNOS, inducible nitric oxide synthase; LPS, lipopolysaccharide; p-, phosphorylated.

ATP-induced ROS production (Fig. 7A and B), alongside its inhibitory effect on MDA and SDH activity (Fig. 7C and D). These results suggested that DI may exert its anti-pyrototic effects by regulating ROS production.

DI inhibits inflammasome-mediated pyroptosis via induction of autophagy. A previous study reported the regulatory effect of autophagy on microglia polarization and the inflammatory process (33). To determine whether DI interfered with autophagy, the protein expression levels of LC3B, ATG-5, Beclin-1 and P62 were analyzed. LC3B-II expression was increased in a concentration-dependent manner and the LC3B-II/LC3B-I ratio was significantly increased following treatment of the cells with 200 μ M DI compared with the

LPS and ATP group. Similarly, Beclin-1 and ATG-5 expression levels were increased, whereas P62 exhibited a tendency toward downregulation following DI treatment (Fig. 8A-E). These data indicated that DI may be involved in the regulation of autophagy.

To confirm the regulatory effect of autophagy on anti-inflammatory activity, the autophagy inhibitor, 3-MA, was used to suppress this process. Cotreatment of the cells with DI and the autophagy inhibitor 3-MA reduced the effects of DI on the expression levels of NLRP3, cleaved GSDMD and IL-1 β , suggesting that DI may regulate cellular anti-inflammatory activity via autophagy (Fig. 8F-J). Taken together, these data indicated that DI exerted anti-inflammatory effects via the induction of autophagy.

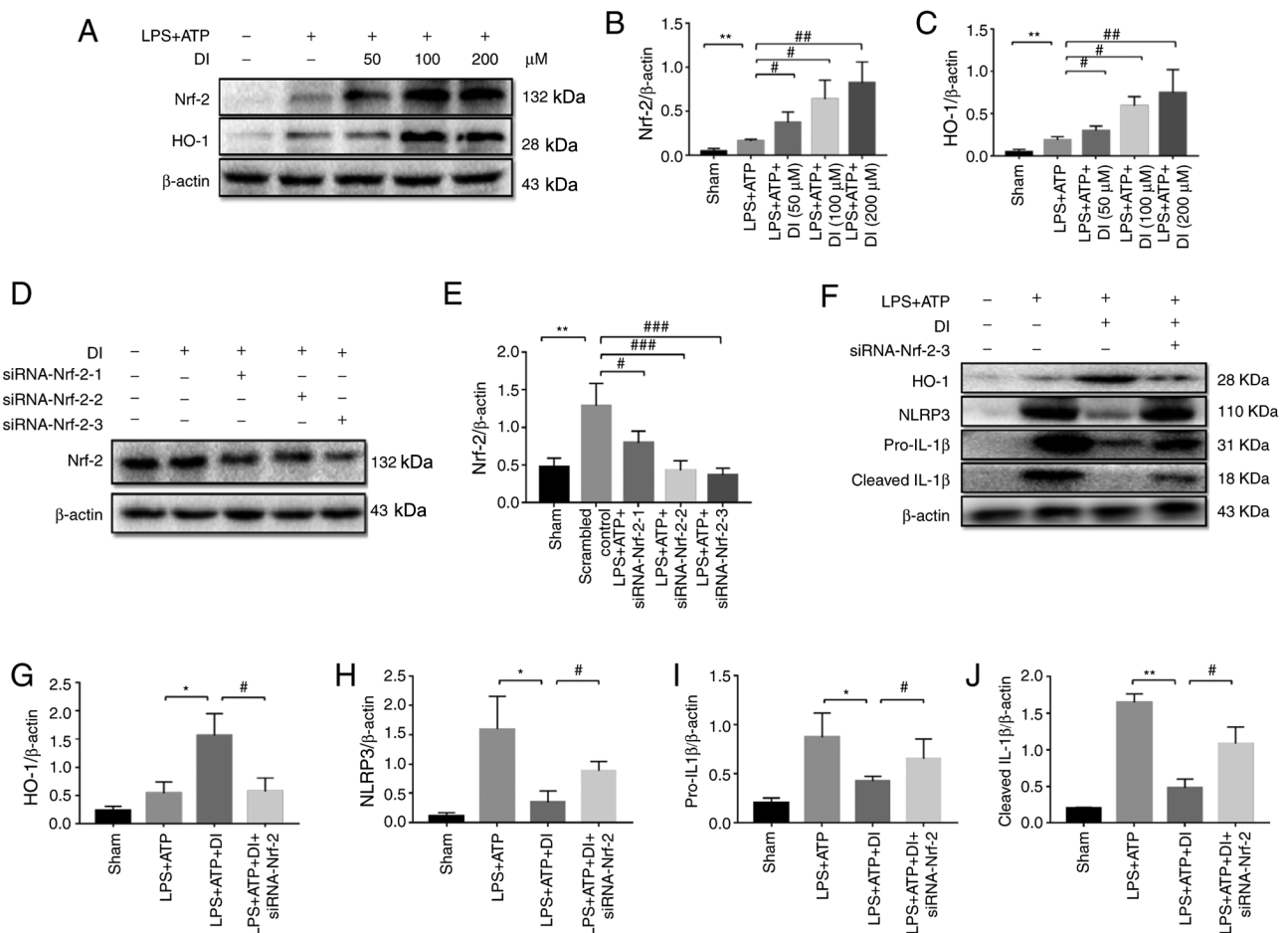


Figure 6. DI positively regulates the Nrf-2/HO-1 pathway. (A) BV2 microglia cells were treated with LPS (1.5 μg/ml) together with various concentrations of DI (50, 100 or 200 μM) for 5 h, with an additional treatment with ATP (3 mM) for 1 h, and western blotting was performed. The protein expression levels of (B) Nrf-2 and (C) HO-1 were semi-quantified. (D) BV2 cells were transfected with siRNA directed against Nrf-2 and western blotting was performed. (E) Protein expression levels of Nrf-2 were semi-quantified. (F) Western blotting was performed after siRNA transfection. Protein expression levels of (G) HO-1, (H) NLRP3, (I) pro-IL-1β and (J) cleaved IL-1β upon siRNA-Nrf-2 transfection were semi-quantified. Data are presented as the mean ± standard error of the mean (n=3). *P<0.05, **P<0.01 vs. sham group or as indicated; #P<0.05, ##P<0.01, ###P<0.001 vs. LPS+ATP group or as indicated. DI, dimethyl itaconate; HO-1, heme oxygenase-1; LPS, lipopolysaccharide; NLRP3, NLR family pyrin domain-containing 3; Nrf-2, nuclear factor erythroid 2-related factor 2; siRNA, small interfering RNA.

Discussion

The present study indicated that DI inhibited the inflammatory response and regulated microglia polarization following stimulation with LPS and ATP. The functions ascribed to DI include inhibition of the NLRP3 inflammasome, stimulation of the antioxidative transcription factor Nrf-2 and regulation of autophagy. The experiments aimed to determine the role of DI in LPS- and ATP-induced pyroptotic microglia. DI effectively attenuated NLRP3 inflammasome assembly and subsequently restrained caspase-1-associated canonical pyroptosis *in vitro*. These data confirmed that DI may activate the Nrf-2/HO-1 signaling pathway to induce antioxidant and anti-inflammatory activities. Notably, inhibition of autophagy reversed the anti-inflammatory function of DI. These results suggested that DI effectively decreased inflammation and NLRP3-associated pyroptosis by modulating the Nrf-2/HO-1 pathway and the induction of autophagy.

Metabolic products affect crucial biological functions. Itaconate has recently been reported to function as an immunomodulator in macrophages (34). Following induction

of inflammation by a specific stimulus, *Irg-1* is activated and promotes the production of itaconate from the TCA cycle by decarboxylating cis-aconitase (35). Macrophage models of inflammation have effectively demonstrated the anti-inflammatory activity of itaconate and increased itaconate synthesis has been shown to occur during macrophage activation. *Irg-1*^{-/-} bone marrow-derived macrophages, which lack the ability to synthesize endogenous itaconate, can release higher levels of cytokines in response to LPS stimulation (23). Notably, itaconate is known to exert its antioxidant activity by targeting SDH, thereby reducing the production of ROS derived from succinate oxidation (23,24); however, using the SDH inhibitor dimethyl malonate did not inhibit IL-1β release in an NLRP3 inflammasome assay (35), indicating that SDH inhibition by itaconate was unlikely to be the main mechanism underlying its anti-inflammatory ability. Several cell-permeable derivatives have been synthesized to achieve efficient intracellular delivery of itaconate (36); DI is produced by esterification of a carboxyl group and reduces the negative charge of itaconate, which increases its electrophilicity and derivative functions (23).

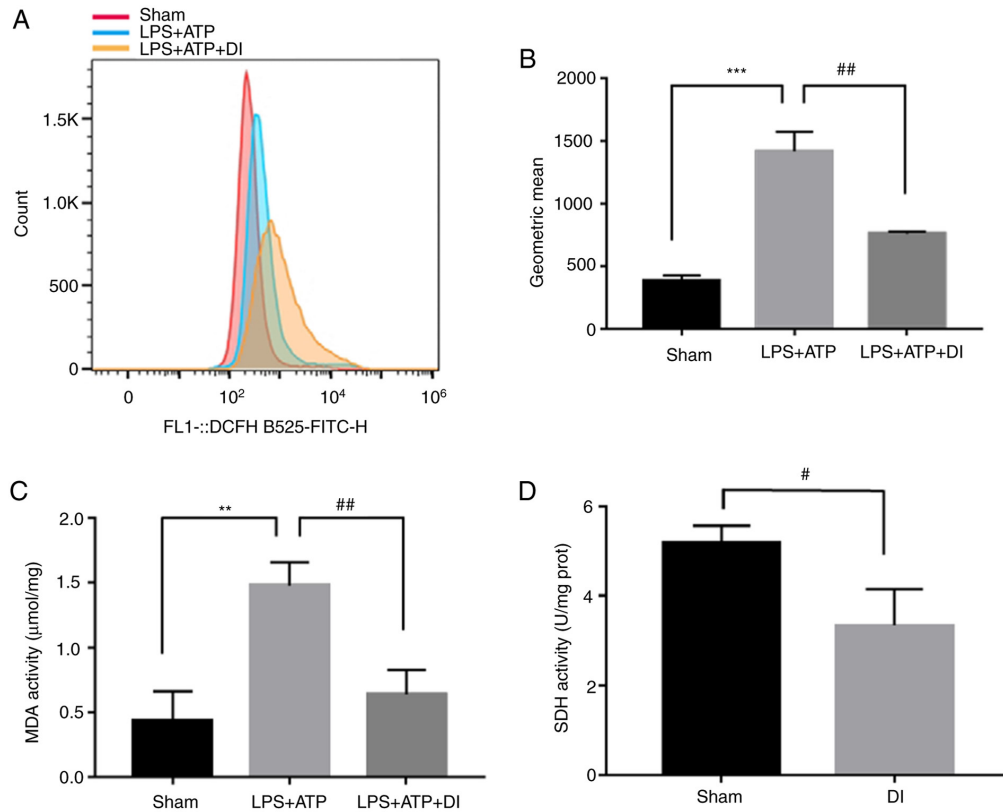


Figure 7. Effects of DI on cellular ROS generation in LPS-activated BV2 microglia. (A and B) BV2 cells were treated with LPS (1.5 μg/ml) together with DI (200 μM) for 5 h, with 1 h additional treatment with ATP (3 mM). Cellular ROS levels were evaluated by flow cytometry using a 2,7-dichlorodihydrofluorescein diacetate probe. (C) MDA activity was measured using a lipid peroxidation MDA assay kit. (D) SDH activity was detected using an SDH assay kit. Data are presented as the mean ± standard error of the mean (n=3). **P<0.01, ***P<0.001 vs. sham group; #P<0.05, ##P<0.01 vs. LPS+ATP group or as indicated. DI, dimethyl itaconate; LPS, lipopolysaccharide; MDA, malondialdehyde; ROS, reactive oxygen species; SDH, succinate dehydrogenase.

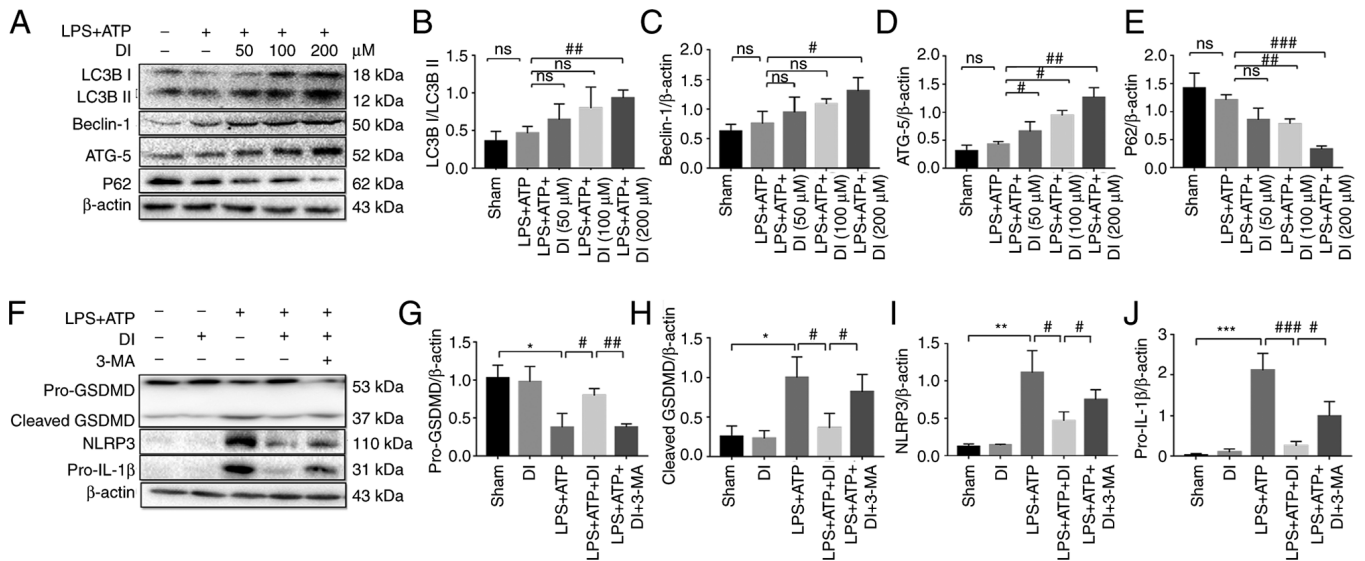


Figure 8. DI inhibits inflammasome-mediated pyroptosis through autophagy. (A) Autophagy markers were detected by western blotting. Protein expression levels of (B) LC3B, (C) Beclin-1, (D) ATG-5 and (E) P62 were semi-quantified. (F) Association between DI-induced autophagy and inflammation was investigated by western blotting. Protein expression levels of (G) GSDMD, (H) cleaved GSDMD, (I) NLRP3 and (J) pro-IL-1β were semi-quantified. Data are presented as the mean ± standard error of the mean (n=3). *P<0.05, **P<0.01, ***P<0.001 vs. sham group; #P<0.05, ##P<0.01, ###P<0.001 vs. LPS+ATP group or as indicated. 3-MA, 3-methyladenine; ATG-5, autophagy-related 5; DI, dimethyl itaconate; GSDMD, gasdermin D; LPS, lipopolysaccharide; NLRP3, NLR family pyrin domain-containing 3.

Microglia are unique resident immune cells in the brain that comprise the first and most important line of immune

defense in the central nervous system (5). The induction of genes that are induced most rapidly by LPS stimulation are

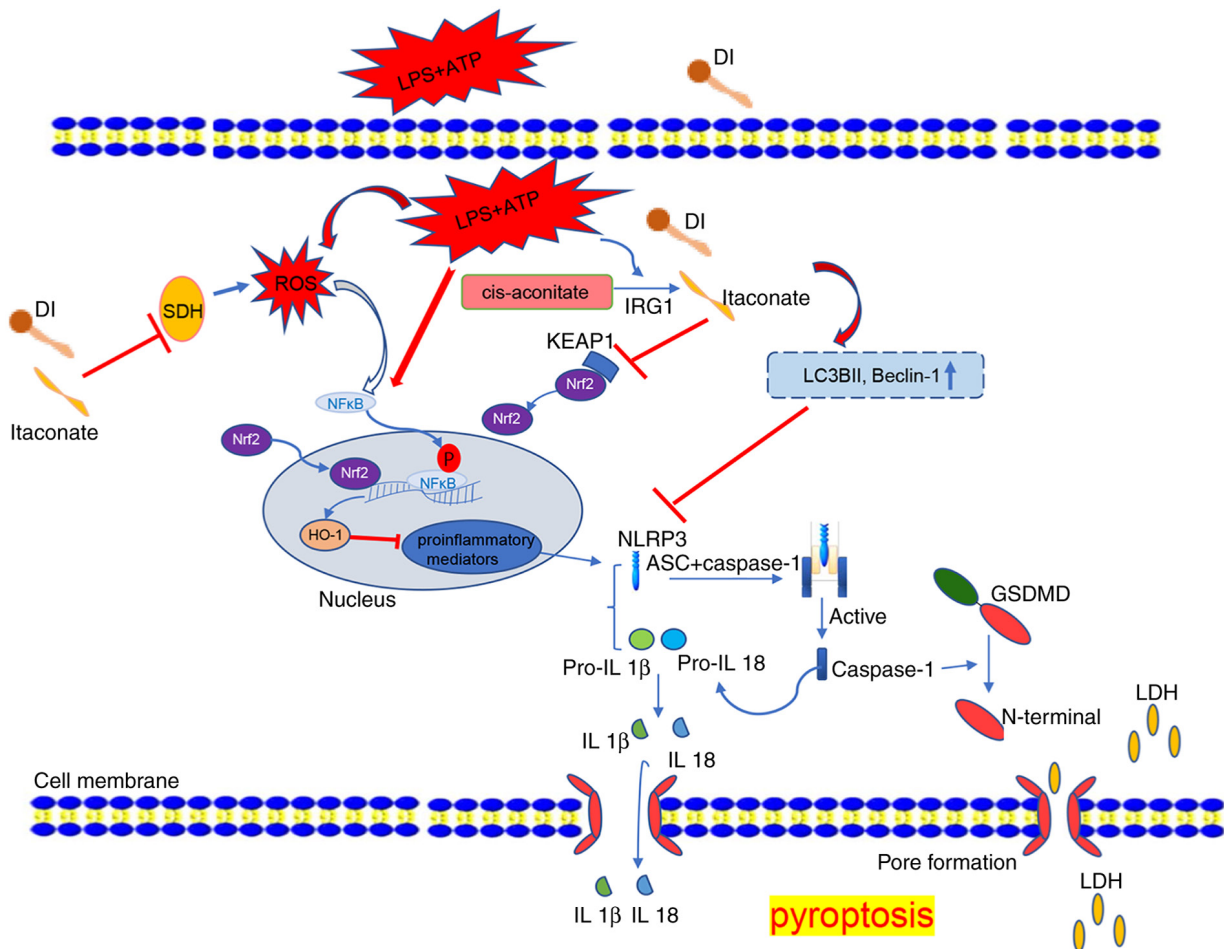


Figure 9. Anti-inflammatory and anti-pyroptotic function of DI in microglia. LPS and ATP induced inflammation and NLRP3 inflammasome-dependent pyroptosis, which also triggered ROS production, NF- κ B phosphorylation and inflammatory mediator expression. DI inhibited SDH activity and induced Nrf2 expression, which subsequently induced HO-1 to inhibit pro-inflammatory mediator induction. DI inhibited NLRP3 inflammasome and triggered autophagy to inhibit NLRP3 inflammasome assembly, eventually blocking GSDMD pore formation and IL-1 β secretion. DI, dimethyl itaconate; GSDMD, gasdermin D; HO-1, heme oxygenase-1; IRG1, immune responsive gene 1; KEAP1, Kelch-like ECH-associated protein 1; LDH, lactate dehydrogenase; LPS, lipopolysaccharide; NLRP3, NLR family pyrin domain-containing 3; ROS, reactive oxygen species; SDH, succinate dehydrogenase.

known as the primary response, such as TNF- α ; while the induction of secondary response genes require chromatin remodeling as a prerequisite for transcription factor binding and the recruitment of histone-modifying enzymes and the general transcription initiation machinery (37). The findings of the present study indicated that treatment of microglia with DI inhibited their primary and secondary transcriptional response to LPS. Moreover, LPS-stimulated microglia M1 polarization was reduced with DI treatment. However, exogenous addition of the itaconate derivative did not result in metabolic production of endogenous itaconate (38). As a more powerful version of itaconate, the dimethyl derivative exhibits increased electrophilicity that may not truly reflect the innate biological function of the endogenous compound. Irg-1 is the key protein that produces intracellular itaconate, so knockdown of *Irg-1* could fundamentally impair itaconate production, which could be helpful to investigate the true biological function of itaconate (25). Therefore, the *Irg-1*^{-/-} microglia model should be utilized for subsequent investigations.

It is now generally accepted that NLRP3 inflammasome signaling serves a critical role in the pathogenesis of several

neurological diseases, including traumatic brain injury, ischemic stroke and neurodegenerative diseases (39,40). Following stimulation by PAMPs and/or DAMPs, microglia are activated and release a series of inflammatory mediators, including NLR-inflammasome members and specific cytokines (7). Hooftman *et al* (35) revealed that the metabolite itaconate specifically suppressed NLRP3 inflammasome activation by reducing the NLRP3-NEK7 interaction and modulating C548 on NLRP3, eventually resulting in blockage of IL-1 β release, which may account for the intrinsic molecular mechanism of its anti-inflammatory ability (35). In the present study, external administration of DI effectively reduced NLRP3 inflammasome activation and subsequently inhibited NLRP3-mediated GSDMD cleavage, further emphasizing the inhibitory effect of DI on pyroptosis. The previous studies performed by our group highlighted the importance of inhibiting the NLRP3 inflammasome in order to achieve neural functional recovery from traumatic injury and ischemia stroke (41-43). DI may possess significant potential as a neuropathological drug for promoting neurological functional recovery due to its strong inhibitory activity against NLRP3-mediated pathways.

NLRP3 mediates the canonical pyroptotic pathway in microglia, which is characterized by cellular membrane perforation and disintegration, and eventually results in cell lysis (44). Canonical pyroptosis elicits NLRP3 inflammasome assembly, activation of caspase-1, cleavage and formation of GSDMD pores, and release of mature IL-18 and IL-1 β (45). The formation of the GSDMD pore leads to disrupted osmotic potential and cell swelling (13,20). In the present study, LPS- and ATP-mediated stimulation of microglia was used to trigger intracellular pyroptosis *in vitro*. LDH release occurs following the activation of GSDMD expression, which is accompanied by increased expression of cleaved caspase-1 and subsequent inhibition of GSDMD cleavage (46). Simultaneously, LPS- and ATP-mediated stimulation of microglia also induced M1 polarization, which released pro-inflammatory cytokines and increased NLRP3 expression. This triggered NLRP3-mediated pyroptosis. DI effectively facilitated the transition from M1 to M2, which in turn blocked NLRP3-mediated canonical pyroptosis.

To further elucidate the mechanism by which DI attenuated inflammation, the Nrf-2/HO-1 pathway was assessed. It is widely recognized that Nrf-2 is a transcription factor that regulates the inflammatory response and the induction of oxidative stress (28). Nrf-2 induces the expression of numerous proteins that are released in response to cytotoxic effects, oxidative stress and inflammation. Xu *et al* (47) reported that Nrf-2 ameliorated inflammation by inducing HO-1 expression, which resulted in downregulation of TNF- α expression. Moreover, Nrf-2 can directly bind to the promoter region of IL-6 and IL-1 β . Under normal conditions, Nrf-2 is covalently bound to KEAP1, whereas itaconate can effectively reduce the inhibitory effect on Nrf-2 (28), thus indicating the intrinsic anti-inflammatory mechanism of itaconate. The present study confirmed that DI caused an upregulation in Nrf-2 expression and inhibited LPS-induced inflammatory cytokine levels in microglia. Furthermore, DI inhibited the NF- κ B signaling pathway, which may regulate pro-inflammatory cytokine production. Several studies have shown that activation of the Nrf-2/HO-1 pathway is associated with the NF- κ B signaling pathway (48-50), indicating the anti-inflammatory effect of DI on microglia.

The activation of autophagy can cause or prevent neurological damage. It has been reported that the induction of autophagy can decrease cell death and promote recovery of neurological function (51,52). Therefore, the induction of autophagy may protect microglial cells against LPS- and ATP-induced damage. Previous studies have demonstrated the association between autophagy and inflammatory processes. Wang *et al* (33) demonstrated that macrophage polarization was regulated via LC3-dependent autophagy in *Brucella*. In addition, several reports have concluded that activation of autophagy can prevent pyroptosis (53,54). Notably, the NLRP3 inflammasome can be selectively degraded by autophagy, limiting cytokine secretion and reducing pyroptosis (55,56). In the present study, DI caused a marked increase in LC3B-II, ATG-5 and Beclin-1 expression levels, indicating that it augmented intracellular autophagy levels. Furthermore, a suppressive effect of DI was noted on LPS-induced NLRP3, IL-1 β and cleaved GSDMD expression; this effect was reversed by 3-MA, thus confirming that DI exerted its anti-inflammatory effects partly by activating autophagy.

There are some limitations to the present study. Firstly, apart from NLRs-driven inflammasome assembly, the present study did not assess TLRs, which also trigger the initiation of inflammation and pyroptosis. Secondly, the esterification of a carboxyl group increases the electrophilicity of itaconate, which hides the true biological function of itaconate; therefore, application of lower electrophilic derivatives, such as 4-octyl itaconate, or an *Irg-1*^{-/-} microglia model in further studies would intuitively present the biological function. Thirdly, in the present study, groups were set and experiments were repeated three times; according to acknowledged rules, the sample size (n) should be more than three in *in vitro* cell tests and more than five in *in vivo* animal tests (57). Expanding the sample size would make the statistical analysis more reliable. Despite these limitations, the present study discovered a novel itaconate derivative with prominent anti-inflammatory and anti-pyroptotic activity. Future research may focus on its anti-inflammatory effect *in vivo*.

In conclusion, the results of the present study indicated that DI exerted anti-inflammatory and anti-pyroptotic effects on LPS- and ATP-stimulated microglia. This protective mechanism of DI was associated with inhibition of production of the NLRP3 inflammasome and suppression of inflammatory cytokine release. These effects were mediated by activation of the Nrf-2/HO-1 pathway and the regulation of autophagy. The findings of the present study emphasize the therapeutic potential of DI for neurological diseases. The potential anti-inflammatory and anti-pyroptotic mechanisms of DI in microglia are shown in Fig. 9.

Acknowledgements

Not applicable.

Funding

This research was funded by grants from the National Natural Science Foundation of China (grant nos. 81820108011 and 81771262) and the Wenzhou Municipal Science and Technology Bureau Project (grant nos. Y20190566 and Y20180153).

Availability of data and materials

All data generated or analyzed during this study are included in this published article.

Authors' contributions

SY and LH conceived and designed the experiments, performed the experiments, analyzed the data, contributed reagents/materials/analytical tools, wrote the manuscript, prepared figures and reviewed the manuscript. XZ, XiangL, YZ, XC, HZ and XiaoL performed the experiments, analyzed the data, contributed reagents/materials/analysis tools and prepared figures. QZ conceived and designed the experiments and provided funding. SY and LH confirm the authenticity of all the raw data. All authors read and approved the final manuscript.

Ethics approval and consent to participate

The present study was approved by the Ethics Committee of Wenzhou Medical University (approval no. wydw2019-0598).

Patient consent for publication

Not applicable.

Competing interests

The authors declare that they have no competing interests.

References

1. Dheen ST, Kaur C and Ling EA: Microglial activation and its implications in the brain diseases. *Curr Med Chem* 14: 1189-1197, 2007.
2. Walter L and Neumann H: Role of microglia in neuronal degeneration and regeneration. *Semin Immunopathol* 31: 513-525, 2009.
3. Hu X, Leak RK, Shi Y, Suenaga J, Gao Y, Zheng P and Chen J: Microglial and macrophage polarization-new prospects for brain repair. *Nat Rev Neurol* 11: 56-64, 2015.
4. Lan X, Han X, Li Q, Yang QW and Wang J: Modulators of microglial activation and polarization after intracerebral haemorrhage. *Nat Rev Neurol* 13: 420-433, 2017.
5. Lee E, Eo JC, Lee C and Yu JW: Distinct features of brain-resident macrophages: Microglia and non-parenchymal brain macrophages. *Mol Cells* 44: 281-291, 2021.
6. Xiong XY, Liu L and Yang QW: Functions and mechanisms of microglia/macrophages in neuroinflammation and neurogenesis after stroke. *Prog Neurobiol* 142: 23-44, 2016.
7. Mathur A, Hayward JA and Man SM: Molecular mechanisms of inflammasome signaling. *J Leukoc Biol* 103: 233-257, 2018.
8. Gritsenko A, Green JP, Brough D and Lopez-Castejon G: Mechanisms of NLRP3 priming in inflammaging and age related diseases. *Cytokine Growth Factor Rev* 55: 15-25, 2020.
9. Wang L and Hauenstein AV: The NLRP3 inflammasome: Mechanism of action, role in disease and therapies. *Mol Aspects Med* 76: 100889, 2020.
10. Liu YG, Chen JK, Zhang ZT, Ma XJ, Chen YC, Du XM, Liu H, Zong Y and Lu GC: NLRP3 inflammasome activation mediates radiation-induced pyroptosis in bone marrow-derived macrophages. *Cell Death Dis* 8: e2579, 2017.
11. Sorbara MT and Girardin SE: Mitochondrial ROS fuel the inflammasome. *Cell Res* 21: 558-560, 2011.
12. Gurung P, Lukens JR and Kanneganti TD: Mitochondria: Diversity in the regulation of the NLRP3 inflammasome. *Trends Mol Med* 21: 193-201, 2015.
13. Shi J, Gao W and Shao F: Pyroptosis: Gasdermin-mediated programmed necrotic cell death. *Trends Biochem Sci* 42: 245-254, 2017.
14. Fink SL and Cookson BT: Apoptosis, pyroptosis, and necrosis: Mechanistic description of dead and dying eukaryotic cells. *Infect Immun* 73: 1907-1916, 2005.
15. Sarhan M, Land WG, Tonnus W, Hugo CP and Linkermann A: Origin and consequences of necroinflammation. *Physiol Rev* 98: 727-780, 2018.
16. Tang D, Kang R, Berghe TV, Vandenabeele P and Kroemer G: The molecular machinery of regulated cell death. *Cell Res* 29: 347-364, 2019.
17. He Y, Hara H and Nunez G: Mechanism and regulation of NLRP3 inflammasome activation. *Trends Biochem Sci* 41: 1012-1021, 2016.
18. Weigt SS, Palchevskiy V and Belperio JA: Inflammasomes and IL-1 biology in the pathogenesis of allograft dysfunction. *J Clin Invest* 127: 2022-2029, 2017.
19. Kovacs SB and Miao EA: Gasdermins: Effectors of pyroptosis. *Trends Cell Biol* 27: 673-684, 2017.
20. Liu X, Zhang Z, Ruan J, Pan Y, Magupalli VG, Wu H and Lieberman J: Inflammasome-activated gasdermin D causes pyroptosis by forming membrane pores. *Nature* 535: 153-158, 2016.
21. Dempsey LA: Immunoregulatory itaconate. *Nat Immunol* 19: 511, 2018.
22. Yu XH, Zhang DW, Zheng XL and Tang CK: Itaconate: An emerging determinant of inflammation in activated macrophages. *Immunol Cell Biol* 97: 134-141, 2019.
23. Lampropoulou V, Sergushicheva E, Bambouskova M, Nair S, Vincent EE, Loginicheva E, Cervantes-Barragan L, Ma X, Huang SC, Griss T, *et al*: Itaconate links inhibition of succinate dehydrogenase with macrophage metabolic remodeling and regulation of inflammation. *Cell Metab* 24: 158-166, 2016.
24. Bordon Y: Itaconate charges down inflammation. *Nat Rev Immunol* 18: 360-361, 2018.
25. Cordes T, Wallace M, Michelucci A, Divakaruni AS, Sapcaru SC, Sousa C, Koseki H, Cabrales P, Murphy AN, Hiller K and Metallo CM: Immunoresponse gene 1 and itaconate inhibit succinate dehydrogenase to modulate intracellular succinate levels. *J Biol Chem* 291: 14274-14284, 2016.
26. Zhao C, Jiang P, He Z, Yuan X, Guo J, Li Y, Hu X, Cao Y, Fu Y and Zhang N: Dimethyl itaconate protects against lipopolysaccharide-induced mastitis in mice by activating MAPKs and Nrf2 and inhibiting NF-kappaB signaling pathways. *Microb Pathog* 133: 103541, 2019.
27. Shan Q, Li X, Zheng M, Lin X, Lu G, Su D and Lu X: Protective effects of dimethyl itaconate in mice acute cardiotoxicity induced by doxorubicin. *Biochem Biophys Res Commun* 517: 538-544, 2019.
28. Mills EL, Ryan DG, Prag HA, Dikovskaya D, Menon D, Zaslona Z, Jedrychowski MP, Costa ASH, Higgins M, Hams E, *et al*: Itaconate is an anti-inflammatory metabolite that activates Nrf2 via alkylation of KEAP1. *Nature* 556: 113-117, 2018.
29. Perico L, Wyatt CM and Benigni A: A new BEACON of hope for the treatment of inflammation? The endogenous metabolite itaconate as an alternative activator of the KEAP1-Nrf2 system. *Kidney Int* 94: 646-649, 2018.
30. Livak KJ and Schmittgen TD: Analysis of relative gene expression data using real-time quantitative PCR and the 2(-Delta Delta C(T)) method. *Methods* 25: 402-408, 2001.
31. Tang C, Wang X, Xie Y, Cai X, Yu N, Hu Y and Zheng Z: 4-Octyl itaconate activates Nrf2 signaling to inhibit pro-inflammatory cytokine production in peripheral blood mononuclear cells of systemic lupus erythematosus patients. *Cell Physiol Biochem* 51: 979-990, 2018.
32. Abais JM, Xia M, Zhang Y, Boini KM and Li PL: Redox regulation of NLRP3 inflammasomes: ROS as trigger or effector? *Antioxid Redox Signal* 22: 1111-1129, 2015.
33. Wang Y, Li Y, Li H, Song H, Zhai N, Lou L, Wang F, Zhang K, Bao W, Jin X, *et al*: Brucella dysregulates monocytes and inhibits macrophage polarization through LC3-dependent autophagy. *Front Immunol* 8: 691, 2017.
34. Li R, Zhang P, Wang Y and Tao K: Itaconate: A metabolite regulates inflammation response and oxidative stress. *Oxid Med Cell Longev* 2020: 5404780, 2020.
35. Hooftman A, Angiari S, Hester S, Corcoran SE, Runtz MC, Ling C, Ruzek MC, Slivka PF, McGettrick AF, Banahan K, *et al*: The immunomodulatory metabolite itaconate modifies NLRP3 and inhibits inflammasome activation. *Cell Metab* 32: 468-478, e7, 2020.
36. Sano M, Tanaka T, Ohara H and Aso Y: Itaconic acid derivatives: Structure, function, biosynthesis, and perspectives. *Appl Microbiol Biotechnol* 104: 9041-9051, 2020.
37. Medzhitov R and Horng T: Transcriptional control of the inflammatory response. *Nat Rev Immunol* 9: 692-703, 2009.
38. Sun KA, Li Y, Meliton AY, Woods PS, Kimmig LM, Cetin-Atalay R, Hamanaka RB and Mutlu GM: Endogenous itaconate is not required for particulate matter-induced NRF2 expression or inflammatory response. *Elife* 9: e54877, 2020.
39. Fusco R, Siracusa R, Genovese T, Cuzzocrea S and Di Paola R: Focus on the role of NLRP3 inflammasome in diseases. *Int J Mol Sci* 21: 2020.
40. Song L, Pei L, Yao S, Wu Y and Shang Y: NLRP3 Inflammasome in Neurological Diseases, from Functions to Therapies. *Front Cell Neurosci* 11: 63, 2017.
41. Wang K, Sun Z, Ru J, Wang S, Huang L, Ruan L, Lin X, Jin K, Zhuge Q and Yang S: Ablation of GSDMD improves outcome of ischemic stroke through blocking canonical and non-canonical inflammasomes dependent pyroptosis in microglia. *Front Neurol* 11: 577927, 2020.

42. Wang K, Ru J, Zhang H, Chen J, Lin X, Lin Z, Wen M, Huang L, Ni H, Zhuge Q and Yang S: Melatonin enhances the therapeutic effect of plasma exosomes against cerebral ischemia-induced pyroptosis through the TLR4/NF- κ B pathway. *Front Neurosci* 14: 848, 2020.
43. Sun Z, Nyanzu M, Yang S, Zhu X, Wang K, Ru J, Yu E, Zhang H, Wang Z, Shen J, *et al*: VX765 attenuates pyroptosis and HMGB1/TLR4/NF-kappaB pathways to improve functional outcomes in TBI mice. *Oxid Med Cell Longev* 2020: 7879629, 2020.
44. Orning P, Lien E and Fitzgerald KA: Gasdermins and their role in immunity and inflammation. *J Exp Med* 216: 2453-2465, 2019.
45. Schroder K and Tschopp J: The inflammasomes. *Cell* 140: 821-832, 2010.
46. Gaidt MM and Hornung V: Pore formation by GSDMD is the effector mechanism of pyroptosis. *EMBO J* 35: 2167-2169, 2016.
47. Xu M, Jiang P, Sun H, Yuan X, Gao S, Guo J, Zhao C, Hu X, Liu X and Fu Y: Dimethyl itaconate protects against lipopolysaccharide-induced endometritis by inhibition of TLR4/NF-kappaB and activation of Nrf2/HO-1 signaling pathway in mice. *Iran J Basic Med Sci* 23: 1239-1244, 2020.
48. Shalaby YM, Menze ET, Azab SS and Awad AS: Involvement of Nrf2/HO-1 antioxidant signaling and NF-kappaB inflammatory response in the potential protective effects of vincamine against methotrexate-induced nephrotoxicity in rats: Cross talk between nephrotoxicity and neurotoxicity. *Arch Toxicol* 93: 1417-1431, 2019.
49. Kim HN, Park GH, Park SB, Kim JD, Eo HJ, Son HJ, Song JH and Jeong JB: *Sageretia thea* inhibits inflammation through suppression of NF- κ B and MAPK and activation of Nrf2/HO-1 signaling pathways in RAW264.7 cells. *Am J Chin Med* 47: 385-403, 2019.
50. Subedi L, Lee JH, Yumnam S, Ji E and Kim SY: Anti-inflammatory effect of sulforaphane on LPS-activated microglia potentially through JNK/AP-1/NF- κ B inhibition and Nrf2/HO-1 activation. *Cells* 8: 194, 2019.
51. Harris H and Rubinsztein DC: Control of autophagy as a therapy for neurodegenerative disease. *Nat Rev Neurol* 8: 108-117, 2011.
52. Cadwell K: Crosstalk between autophagy and inflammatory signalling pathways: Balancing defence and homeostasis. *Nat Rev Immunol* 16: 661-675, 2016.
53. Tu Y, Guo C, Song F, Huo Y, Geng Y, Guo M, Bao H, Wu X and Fan W: Mild hypothermia alleviates diabetes aggravated cerebral ischemic injury via activating autophagy and inhibiting pyroptosis. *Brain Res Bull* 150: 1-12, 2019.
54. Li MY, Zhu XL, Zhao BX, Shi L, Wang W, Hu W, Qin SL, Chen BH, Zhou PH, Qiu B, *et al*: Adrenomedullin alleviates the pyroptosis of Leydig cells by promoting autophagy via the ROS-AMPK-mTOR axis. *Cell Death Dis* 10: 489, 2019.
55. Mehto S, Jena KK, Nath P, Chauhan S, Kolapalli SP, Das SK, Sahoo PK, Jain A, Taylor GA and Chauhan S: The Crohn's disease risk factor IRGM limits NLRP3 inflammasome activation by impeding its assembly and by mediating its selective autophagy. *Mol Cell* 73: 429-445 e427, 2019.
56. Shi CS, Shenderov K, Huang NN, Kabat J, Abu-Asab M, Fitzgerald KA, Sher A and Kehrl JH: Activation of autophagy by inflammatory signals limits IL-1 β production by targeting ubiquitinated inflammasomes for destruction. *Nat Immunol* 13: 255-263, 2012.
57. Marino MJ: The use and misuse of statistical methodologies in pharmacology research. *Biochem Pharmacol* 87: 78-92, 2014.



This work is licensed under a Creative Commons Attribution-NonCommercial-NoDerivatives 4.0 International (CC BY-NC-ND 4.0) License.